Modeling of Conductor Loss in Coplanar Circuit Elements by the Method of Lines

Larissa Vietzorreck, *Member, IEEE,* and Wilfrid Pascher, *Member, IEEE*

***Abstract*— The small dimensions of coplanar waveguides (CPW's) require due consideration of finite conductivity and metallization thickness. For this purpose, an efficient method of lines (MoL) approach for full-wave analysis of microstrip discontinuities is considerably extended. Two alternative models for the conductor loss are employed depending on the skin depth. Their respective region of validity is investigated and the current distribution in the center conductor of a CPW is given. Several cascaded discontinuities including a coplanar quarter-wave transformer and a short-end series stub in a microshield line are characterized.**

***Index Terms*—Coplanar waveguides, discontinuities, finite conductivity, finite difference methods, method of lines, resistive boundary condition.**

I. Introduction

COPLANAR waveguides (CPW's) have received increasing attention as they possess several advantages over the conventional microstrip lines for monolithic microwave integrated circuit (MMIC) applications. However, finite conductivity and metallization thickness strongly affect the electrical performance of a CPW circuit when the transverse dimensions are of the order of the skin depth. The propagation characteristics of various lossy CPW transmission lines have been previously investigated [1]–[3]. In order to achieve high-performance low-cost CPW components, an accurate full-wave analysis of composite structures containing discontinuities and/or three–dimensional (3-D) elements is necessary. Single discontinuities with perfectly conducting metallization of finite thickness have been analyzed [4], [5], but only few papers (e.g., [6]) have taken the conductor loss of cascaded discontinuities into account.

In recent publications, various planar transmission lines have been investigated using the method of lines (MoL) [7], [8], mostly employing a one-dimensional (1-D) discretization. Losses and finite conductor thickness have been considered for longitudinally homogeneous lines [9], [10]. Another MoL approach using a two-dimensional (2-D) discretization dealt with the investigation of CPW discontinuities, assuming thin and perfect conductors [11]. This approach was restricted to simple structures consisting of a few steps, because of the perpendicular orientation of the discretization lines to the substrate. Recently, an efficient algorithm has been developed for investigation of 3-D microstrip discontinuities [12]. The discretization of the cross section combined with an analytical calculation in propagation direction makes this approach very well suited for treatment of cascaded elements.

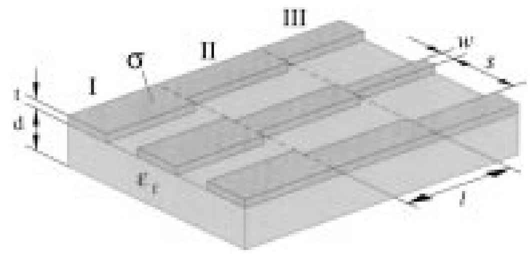

Fig. 1. Cascaded CPW element.

In this paper, cascaded coplanar discontinuities (see Fig. 1) are analyzed using two alternative models for finite conductivity. In the first model, the conductor losses are incorporated using a self-consistent description of the conductor as a dielectric medium with a large imaginary part of the permittivity [1]. Unlike the longitudinally homogeneous lines [9], [10], a 2-D discretization of the cross section is necessary for the analysis of discontinuities. This model is very well suited for the analysis of structures with metallization thickness larger or commensurate with the skin depth.

The second model is used in case of a very thin metallization (e.g. evaporated gold films of 200-nm thickness) where the thickness is less than the skin depth. The full discretization of such thin strips would severely and unnecessarily increase the required memory and computation time. The skin effect is irrelevant and the electrical field can be treated as homogeneous inside the metallic strips. Under these assumptions, resistive boundary conditions [13], [14] are valid and are used to model the electromagnetic field. The most important feature of this new approach is the introduction of modified difference operators.

II. Theory

In the recently introduced approach for the analysis of cascaded microstrip discontinuities, the metallic strips are considered as perfect conductors [12]. They are excluded from the solution domain and from discretization. Hence, the difference operators are reduced and the surfaces of the strips are regarded as electric walls.

However, in the first conductor model based on the complex permittivity, not only the air and the substrate, but also the whole cross section of the conductors is discretized. Therefore,

Manuscript received March 31, 1997; revised August 15, 1997. This work was supported under a grant from the Deutsche Forschungsgemeinschaft.

The authors are with FernUniversität Hagen, Allgemeine und Theoretische Elektrotechnik, D-58084 Hagen, Germany (e-mail: Larissa.Vietzorreck @FernUni-Hagen.de).

Publisher Item Identifier S 0018-9480(97)08322-1.

the interfaces metal–air and metal–substrate are also treated as dielectric interfaces. The field and the current distribution are calculated inside the metallic strip, which may be arbitrarily thick. The difference operators are established for every point in the cross section and no reduction takes place. This rigorous approach considers the skin-effect correctly.

In the second conductor model, we assume a very small conductor thickness. The surface current density is proportional to the tangential electric field. As a consequence, the electric and magnetic field components are coupled with each other and fulfill resistive boundary conditions [13]. As in the case of perfect conductors, the strips themselves are excluded from the solution domain and the difference operators are reduced. Additionally, novel boundary conditions at the strips cause a modification of the corresponding elements of the difference operators.

In the following analysis, we first summarize the general potential and field equations valid for perfect conductors as well as for the two loss models. Then we use resistive boundary conditions to establish the novel modified difference operators for the loss model using thin conductors.

A. Basic Equations

In each longitudinally homogeneous section, the electromagnetic field is derived from a vector potential $\mathbf{\Pi}$:

$$\mathbf{\Pi} = \phi_x \cdot \mathbf{e}_x + \phi_y \cdot \mathbf{e}_y \tag{1}$$

where ϕ_x and ϕ_y fulfill coupled differential equations of the Sturm–Liouville type [8], [12]:

$$\frac{\partial^2}{\partial z^2}\phi_x + \frac{\partial^2}{\partial y^2}\phi_x + \varepsilon_r \frac{\partial}{\partial x}\left(\varepsilon_r^{-1}\left(\frac{\partial \phi_x}{\partial x} + \frac{\partial \phi_y}{\partial y}\right)\right) + \varepsilon_r k_0^2 \phi_x - \frac{\partial}{\partial y}\left(\frac{\partial \phi_y}{\partial x}\right) = 0 \tag{2}$$

$$\frac{\partial^2}{\partial z^2}\phi_y + \frac{\partial^2}{\partial x^2}\phi_y + \varepsilon_r \frac{\partial}{\partial y}\left(\varepsilon_r^{-1}\left(\frac{\partial \phi_y}{\partial y} + \frac{\partial \phi_x}{\partial x}\right)\right) + \varepsilon_r k_0^2 \phi_y - \frac{\partial}{\partial x}\left(\frac{\partial \phi_x}{\partial y}\right) = 0. \tag{3}$$

The electromagnetic field components are given by

$$H_x = \frac{-\partial \phi_y}{\partial z} \tag{4}$$

$$H_y = \frac{\partial \phi_x}{\partial z} \tag{5}$$

$$H_z = \frac{\partial \phi_y}{\partial x} - \frac{\partial \phi_x}{\partial y} \tag{6}$$

$$E_x = -j\frac{\eta_0}{k_0}\left[\frac{\partial}{\partial x}\left(\varepsilon_r^{-1}\mathrm{div}\mathbf{\Pi}\right) + k_0^2 \phi_x\right] \tag{7}$$

$$E_y = -j\frac{\eta_0}{k_0}\left[\frac{\partial}{\partial y}\left(\varepsilon_r^{-1}\mathrm{div}\mathbf{\Pi}\right) + k_0^2 \phi_y\right] \tag{8}$$

$$E_z = -j\frac{\eta_0}{k_0}\left[\frac{\partial}{\partial_z}\left(\varepsilon_r^{-1}\mathrm{div}\mathbf{\Pi}\right)\right] \tag{9}$$

where a free-space wavenumber k_0, and a free-space impedance η_0 have been assumed.

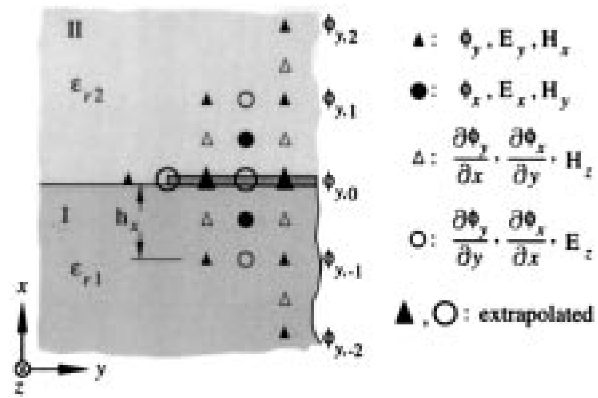

Fig. 2. Discretization scheme of the cross section near a metallic strip with four different line systems: •, ∘, ▲, △.

The cross section of each section is now subjected to a 2-D discretization, the solution in propagation direction being analytical. For simplicity, only equidistant discretization is used to demonstrate the analysis. However, nonequidistant discretization is employed in the computer algorithm. We use four different line systems for the potentials ϕ_x and ϕ_y and their derivatives (see Fig. 2).

The derivatives are determined by means of difference operators, e.g.,

$$\frac{\partial \phi_y}{\partial x} \longrightarrow \boldsymbol{D}_x \boldsymbol{\Phi}_y \tag{10}$$

with

$$\boldsymbol{D}_x = \left[\begin{array}{cccc|cccc} -1 & 1 & & & & & & \\ & \ddots & \ddots & & & & & \\ & & -1 & 1 & & \mathbf{0} & & \\ & & & -1 & & & & \\ \hline & & & & 1 & & & \\ & \mathbf{0} & & & -1 & 1 & & \\ & & & & & \ddots & \ddots & \\ & & & & & & -1 & 1 \end{array}\right] \tag{11}$$

near a perfectly conducting metallic strip.

B. Resistive Boundary Conditions

In the following analysis, we shall establish these difference operators for cross sections containing thin lossy metallic strips. We need appropriate boundary conditions for the components ϕ_x and ϕ_y of the Hertz potential at the strips. For thin conductors the following resistive boundary conditions

$$\begin{bmatrix} J_y \\ J_z \end{bmatrix} = \begin{bmatrix} H_z^{\mathrm{I}} - H_z^{\mathrm{II}} \\ H_y^{\mathrm{II}} - H_y^{\mathrm{I}} \end{bmatrix} = \sigma t \begin{bmatrix} E_y \\ E_z \end{bmatrix} \tag{12}$$

with the strip thickness t and the conductivity σ hold. Additionally, E_y, E_z, H_x, and ϕ_y are continuous at the conducting strips.

First the modified difference operator $\boldsymbol{D}_x^{\mathrm{mod}}$ for computing $\partial\phi_y/\partial x$ near the strip is derived. It is needed for both differential equations (2) and (3) and for H_z. For the evaluation of $\partial\phi_y/\partial x$, the value of ϕ_y at the strip, namely $\phi_{y,0}$ (see Fig. 2) is necessary. Since the metallic strip is treated as a resistive wall at $x = 0$ and excluded from the solution domain, we do not know the value $\phi_{y,0}$ and we have to use the resistive boundary condition (12) to determine it. Expressing the magnetic field components in (12) by means of the Hertz potential through (5) and (6) yields

$$\frac{\partial}{\partial_z}\left(\phi_x^{\mathrm{II}} - \phi_x^{\mathrm{I}}\right) = \sigma t E_z \qquad (13)$$

$$-\left(\frac{\partial \phi_y^{\mathrm{II}}}{\partial x} - \frac{\partial \phi_y^{\mathrm{I}}}{\partial x}\right) + \left(\frac{\partial \phi_x^{\mathrm{II}}}{\partial y} - \frac{\partial \phi_x^{\mathrm{I}}}{\partial y}\right) = \sigma t E_y. \qquad (14)$$

To eliminate the electric field components, we take the derivative of (13) with respect to y and substitute it into (14) using (8) and (9). To take into account the derivative with respect to z the forward and backward propagating waves are considered separately. As the result is exactly the same for both waves, it is also valid for any linear combination. All the terms containing ϕ_x and $\mathrm{div}\mathbf{\Pi}$ cancel and we obtain

$$\left.\frac{\partial \phi_y^{\mathrm{II}}}{\partial x}\right|_{x=0} - \left.\frac{\partial \phi_y^{\mathrm{I}}}{\partial x}\right|_{x=0} = jk_0\eta_0\sigma t\phi_{y,0}. \qquad (15)$$

As the derivative $\partial\phi_y^{\mathrm{II}}/\partial x$ is not known at $x = 0$, it must be linearly extrapolated from the values $\phi_{y,1}$ and $\phi_{y,2}$ (on the grid points ▲ in Fig. 2) together with the still unknown $\phi_{y,0}$ (indicated by a larger symbol). Similarly $\partial\phi_y^{\mathrm{I}}/\partial x$ is determined. Thus, employing a linear extrapolation of $\partial\phi_y/\partial x$ above and below the strip, we derive a finite-difference expression for the left-hand side of (15), which finally yields the extrapolated potential on the metallic strip as follows:

$$\phi_{y,0} = -K\phi_{y,2} + 4K\phi_{y,1} + 4K\phi_{y,-1} - K\phi_{y,-2} \qquad (16)$$

with

$$K = \frac{1}{6 + j2\sigma t\eta_0 h_x k_0}. \qquad (17)$$

With this expression we are able to fill in the missing values in the modified difference operator $\boldsymbol{D}_x^{\mathrm{mod}}$ used for $\mathbf{\Phi}_y$, shown in (18), at the bottom of the page.

In the next step, we need $\varepsilon_r^{-1}\mathrm{div}\mathbf{\Pi}$ on the strip for computing E_x at $x = \pm h_x/2$ and E_y near the edges of the strip. The calculation is done via E_z using (9). We use a linear extrapolation of ϕ_x to obtain ϕ_x^{I} and ϕ_x^{II} at the strip. Inserting the values in (13), we obtain $E_{z,0}$ and also

$$\varepsilon_r^{-1}\mathrm{div}\mathbf{\Pi} = -\frac{jk_0}{2\eta_0\sigma t}[\phi_{x,2} - 3\phi_{x,1} + 3\phi_{x,-1} - \phi_{x,-2}]. \qquad (19)$$

This finite-difference expression is also used for the wave equations (2) and (3). The corresponding modified difference operator exhibits a similar structure as $\boldsymbol{D}_x^{\mathrm{mod}}$ in (18).

The difference operator for $\partial\phi_x/\partial y$ and the ones derived thereof do not differ from those in the case of perfect conductors because they do not involve any discretization points on the strip.

In the limiting case of perfect conduction, the modified difference operators tend to the unmodified ones; e.g., $\lim_{\sigma\to\infty}\boldsymbol{D}_x^{\mathrm{mod}} = \boldsymbol{D}_x$, which employs a Dirichlet boundary condition at the upper and lower side of the strips. The modification of the difference operators affects all the potential and some of the field equations.

Apart from using the modified difference operators, the solution of the wave equation, the matching procedure, and the cascading of the discontinuities by a generalized scattering-matrix approach are carried out as for perfectly conducting strips [12]. In this way, the approach presented here combines the advantages of the original one [12], especially the analysis of cascaded discontinuities, with the features of advanced modeling for lossy conductors.

III. RESULTS

Using the two alternative conductor models proposed above a great variety of lossy coplanar circuits can be analyzed. To test the validity of the models we discuss some properties for longitudinally homogeneous CPW's before presenting results for several circuit elements.

First, the variation of the attenuation constant α with the conductor thickness t is studied (Fig. 3) and compared with results of a quasi-TEM approach [3]. The results obtained by both models proposed in this paper are presented. For the approximation with resistive boundary conditions and modified difference operators $\boldsymbol{D}_x^{\mathrm{mod}}$, the agreement with [3] is good if the thickness is less than the skin depth $\delta = 0.593$ μm, but the values deviate for $t > \delta$. The model using complex permittivity gives good results also for larger t, but with higher computation time. The whole range of the thickness is covered, combining the two models employed here.

In order to verify the model with complex ε_r, the longitudinal component i_z of the current density is examined. Fig. 4 shows i_z inside the center conductor of a CPW corresponding to Section II in Fig. 5. i_z is given at the two distances y_1, y_2 from the conductor's edge and is normalized to its maximum value i_{z1} at y_1. The difference between the calculated skin depth d_e and the analytical value δ for an unbounded metallic region is less than 10%.

A $\lambda/4$ impedance transformer is chosen as an example for a structure with thick lossy conductors. The influence of the

$$\boldsymbol{D}_x^{\mathrm{mod}} = \left[\begin{array}{cccc|cccc} -1 & 1 & & & & & & \\ & \ddots & \ddots & & & & & \\ & & -1 & 1 & & & & \\ & & K & -1-4K & -4K & K & & \\ \hline & & -K & 4K & 1+4K & -K & & \\ & & & & -1 & 1 & & \\ & & & & & \ddots & \ddots & \\ & & & & & & -1 & 1 \end{array}\right]. \qquad (18)$$

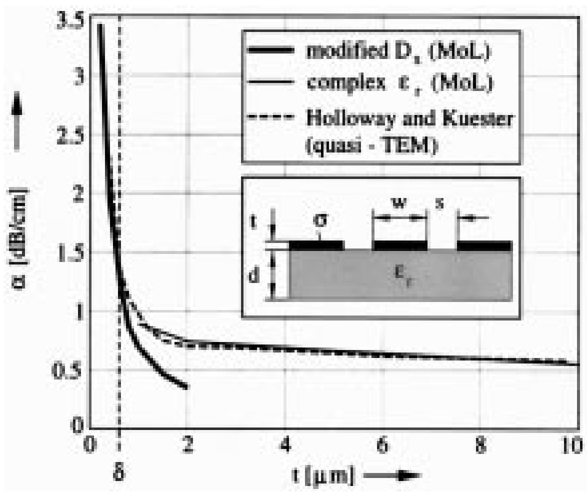

Fig. 3. Variation of attenuation constant α of a CPW as a function of conductor thickness t ($w/2 = 35\ \mu$m, $s = 50\ \mu$m, $\varepsilon_r = 12.9$, $\sigma = 3.602 \cdot 10^7$ S/m, $d = 200\ \mu$m, $f = 20$ GHz).

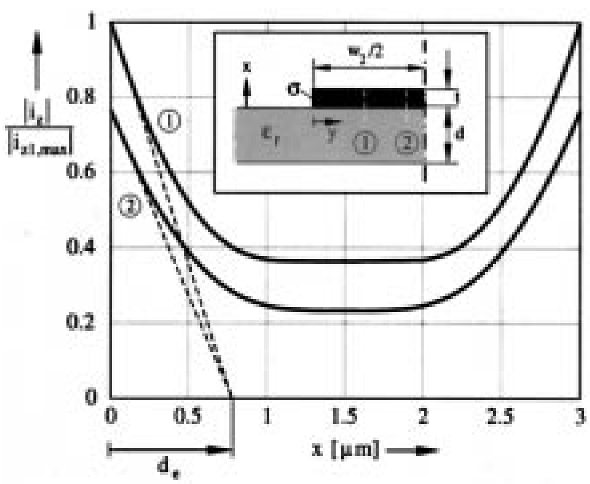

Fig. 4. Longitudinal component i_z of the current density in the center conductor of a CPW at two different positions $y_1 = 2.63\ \mu$m, $y_2 = 6.44\ \mu$m. ($w_2 = 15\ \mu$m, $d = 200\ \mu$m, $\varepsilon_r = 12.9$, $\sigma = 2 \cdot 10^7$ S/m, $t = 3\ \mu$m).

finite conductivity and thickness is clearly seen in the shift of the resonant frequency of the reflection coefficient as well as in the decreasing amplitude of the transmission factor in Fig. 5.

The next example is a microshield short-end series stub (Fig. 6) as proposed in [15]. The ohmic loss of the strips is considered by both methods described in this paper and the resulting scattering parameters are compared to the case of perfect conductors. For lower frequencies, the results for the different models agree very well. For increasing frequency, when the skin depth becomes smaller compared to the conductor thickness, a deviation is visible. However, the performance of the circuit element is much better described by the model using thin lossy conductors than by the simplified model of perfect conductors.

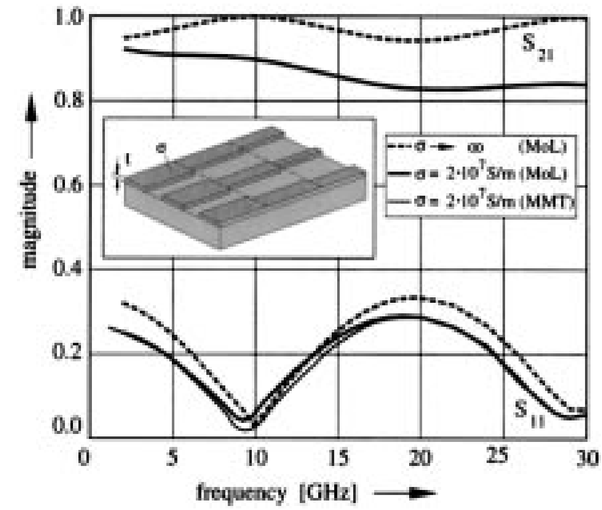

Fig. 5. Magnitude of the scattering parameters of a CPW $\lambda/4$ impedance transformer (see Fig. 1) with lossy and finite conductors compared with results by the mode-matching technique (MMT) [6].($w_1 = 20\ \mu$m, $w_2 = 15\ \mu$m, $w_3 = 8\ \mu$m, $s_1 = 5\ \mu$m, $s_2 = 10\ \mu$m, $s_3 = 17\ \mu$m, $l = 3.104$ mm, $d = 200\ \mu$m, $\varepsilon_r = 12.9$, $\sigma = 2 \cdot 10^7$ S/m, $t = 3\ \mu$m).

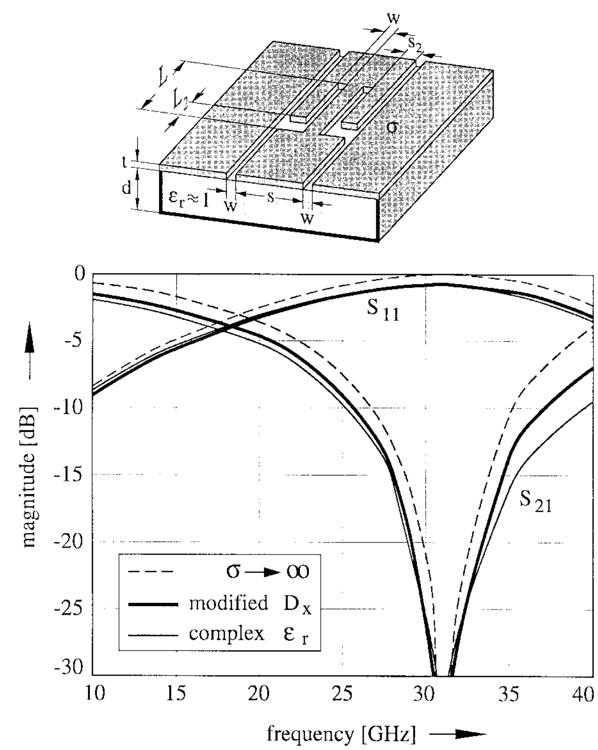

Fig. 6. Magnitude of the scattering parameters of a microshield short-end series stub ($w = 25\ \mu$m, $s = 250\ \mu$m, $s_2 = 80\ \mu$m, $L = 2500\ \mu$m, $L_2 = 200\ \mu$m, $d = 350\ \mu$m, $\varepsilon_r = 1.1$, $\sigma = 3.6 \cdot 10^7$ S/m, $t = 0.5\ \mu$m).

IV. Conclusion

Using the method proposed in this paper, various composite CPW circuit elements are accurately analyzed. Conductor losses, which can severely influence the performance of the circuit, are fully taken into account. It is possible to choose between two different ways of treating the finite conductivity depending on the ratio of the conductor thickness to the skin depth. The first model is based on complex permittivity for comparatively thick conductors. The second one employs the finite sheet admittance of thin conductors to derive special modified difference operators. Since it is not necessary to discretize the small thickness of the metallic strips, an efficient analysis is guaranteed for discontinuities in a great variety of CPW's.

The results for the attenuation constant and for the current density of a CPW prove the validity of both proposed models. The scattering parameters for a coplanar quarter-wave transformer and a short-end series stub in a microshield line computed by different analysis methods show very good agreement.

REFERENCES

[1] W. Heinrich, "Full-wave analysis of conductor losses on MMIC transmission lines," *IEEE Trans. Microwave Theory Tech.*, vol. 38, pp. 1468–1472, Oct. 1990.

[2] S. Hofschen and I. Wolff, "Simulation of an elevated coplanar waveguide using 2-D-FDTD," *IEEE Microwave Guided Wave Lett.*, vol. 6, pp. 28–30, Jan. 1996.

[3] C. Holloway and E. F. Kuester, "A quasi-closed form expression for the conductor loss of CPW lines, with an investigation of edge shape effects," *IEEE Trans. Microwave Theory Tech.*, vol. 43, pp. 2695–2701, Dec. 1995.

[4] T. W. Huang and T. Itoh, "The influence of metallization thickness on the characteristics of cascaded junction discontinuities of shielded coplanar type transmission line," *IEEE Trans. Microwave Theory Tech.*, vol. 41, pp. 693–697, Apr. 1993.

[5] F. Alessandrini, G. Baini, M. Mongiardo, and R. Sorrentino, "A 3-D mode matching technique for the efficient analysis of coplanar MMIC discontinuities with finite metallization thickness," *IEEE Trans. Microwave Theory Tech.*, vol. 41, pp. 1625–1629, Sept. 1993.

[6] R. Schmidt and P. Russer, "Modeling of cascaded coplanar waveguide discontinuities by the mode-matching approach," *IEEE Trans. Microwave Theory Tech.*, vol. 43, pp. 2910–2917, Dec. 1995.

[7] R. Pregla and W. Pascher, "The method of lines," in *Numerical Techniques for Microwave and Millimeter Wave Passive Structures*, T. Itoh, Ed. New York: Wiley, 1989, pp. 381–446.

[8] R. Pregla, "MoL-BPM method of lines based beam propagation method," in *Methods for Modeling and Simulation of Guided-Wave Optoelectronic Devices*, W. P. Huang, Ed. Cambridge, MA: EMW Pub., 1995, pp. 51–102.

[9] F. J. Schmückle and R. Pregla, "The method of lines for the analysis of lossy planar waveguide structures," *IEEE Trans. Microwave Theory Tech.*, vol. 38, pp. 1473–1479, Oct. 1990.

[10] K. Wu, R. Vahldieck, J. L. Fikart, and H. Minkus, "The influence of finite conductor thickness and conductivity on fundamental and higher-order modes in miniature hybrid MIC's (MHMIC's) and MMIC's," *IEEE Trans. Microwave Theory Tech.*, vol. 41, pp. 421–430, Mar. 1993.

[11] S.-J. Chung and T.-R. Chrang, "Full-wave analysis of discontinuities in conductor-backed coplanar waveguides using the method of lines," *IEEE Trans. Microwave Theory Tech.*, vol. 41, pp. 1601–1605, Mar. 1993.

[12] L. Vietzorreck and R. Pregla, "Hybrid analysis of 3-D MMIC elements by the method of lines," *IEEE Trans. Microwave Theory Tech.*, vol. 44, pp. 2580–2586, Dec. 1996.

[13] T. B. A. Senior, "Approximate boundary conditions," *IEEE Trans. Antennas Propagat.*, vol. AP-29, pp. 826–829, Sept. 1981.

[14] R. Pregla, "Comments on: Analysis of the effects of a resistively coated upper dielectric layer on the propagation characteristics of hybrid modes in a waveguide-shielded microstrip using the method of lines," *IEEE Trans. Microwave Theory Tech.*, vol. 42, p. 2013, Oct. 1994.

[15] T. Weller, L. P. B. Kathehi, and G. Rebeiz, "High performance microshield line components," *IEEE Trans. Microwave Theory Tech.*, vol. 43, pp. 534–543, Mar. 1995.

Larissa Vietzorreck (M'96) was born in Düsseldorf, Germany, in 1965. She received the Dipl.-Ing. degree in electrical engineering from the Ruhr-Universität Bochum, Germany, in 1992, and is currently working toward the doctoral degree.

Since 1992, she has been a Research Assistant in the Department of Electrical Engineering, FernUniversität, Hagen, Germany. Her research interests are numerical modeling of planar microwave components and printed antennas.

Wilfrid Pascher (M'95) was born in Graz, Austria, on September 17, 1958. He received the Dipl.-Ing. degree in technical physics from the Technical University Graz, Graz, Austria, in 1984, and the Dr.-Ing. degree from the FernUniversität, Hagen, Germany, in 1990.

From 1985 to 1990, he was a Research Assistant in the Department of Electrical Engineering, FernUniversität, where he was engaged in the investigation of planar and rectangular-waveguide components. Since 1990, he has been a Senior Engineer and is currently involved in waveguide theory and the numerical modeling of passive components for microwaves and electro-optics.